University of South Florida
Scholar Commons

Geology Faculty Publications

Geology

2001

Longshore Sediment Transport as a Function of Energy Dissipation

Ernest R. Smith
U.S. Army Engineer Research and Development Center, smithe@wes.army.mil

Ping Wang
University of South Florida, pwang@usf.edu

LONGSHORE SEDIMENT TRANSPORT AS A FUNCTION OF ENERGY DISSIPATION

Ernest R. Smith[1], M.ASCE, and Ping Wang[2]

Abstract: Experiments to measure waves, currents, and sediment transport rate for two breaker types, plunging and spilling, were conducted in a large-scale three-dimensional physical model. It was found that there was a large difference in cross-shore distribution and total sediment transport rate between the two breaker types. Total transport rates compared to existing predictive equations. The equations generally did not predict the data well. With the exception of the Kamphuis (1991) equation, which included a dependence on wave period, the predictive equations did not differentiate between breaker types.

INTRODUCTION

Total longshore sediment transport rate and its cross-shore distribution in the surf zone are essential to many coastal engineering studies. The U.S. Army Engineer Research and Development Center recently completed a large-scale Longshore Sediment Transport Facility (LSTF) to study longshore sediment transport. The facility has the capability of simulating wave heights that are comparable to annual averages along many low-wave energy coasts, such as many of the beaches along the Gulf of Mexico and the Great Lakes in the U.S. This paper describes the capabilities of the LSTF and presents comparisons to some of the existing predictive equations for longshore sediment transport.

LONGSHORE SEDIMENT TRANSPORT FACILITY

The LSTF was designed to generate waves and currents and conduct sediment transport experiments at a large scale. The facility consists of a 30-m wide, 50-m long, 1.4-m deep basin, and includes four wave generators, a sand beach, a recirculation system, and an instrumentation bridge (Figure 1). The following paragraphs describe the equipment used in the facility.

---

1 Research Hydraulic Engineer, Engineering Research and Development Center, Coastal and Hydraulics Lab, 3909 Halls Ferry Road Vicksburg, MS 39180-6199, smithe@wes.army.mil
2 Department of Geology SCA 528, University of South Florida, Tampa, FL 33620, pwang@chmua1.cas.usf.edul

	Form Approved
Report Documentation Page	OMB No. 0704-0188

1. REPORT DATE **2001**	2. REPORT TYPE **N/A**	3. DATES COVERED **-**

4. TITLE AND SUBTITLE **Longshore Sediment Transport as a Function of Energy Dissipation**	5a. CONTRACT NUMBER
	5b. GRANT NUMBER
	5c. PROGRAM ELEMENT NUMBER
6. AUTHOR(S) **Ernest R. /Smith; Ping /Wang**	5d. PROJECT NUMBER
	5e. TASK NUMBER
	5f. WORK UNIT NUMBER

7. PERFORMING ORGANIZATION NAME(S) AND ADDRESS(ES) **Coastal and Hydraulics Laboratory - Engineer Research and Development Center Waterways Experiment Station - Vicksburg, Mississippi**	8. PERFORMING ORGANIZATION REPORT NUMBER

9. SPONSORING/MONITORING AGENCY NAME(S) AND ADDRESS(ES)	10. SPONSOR/MONITOR'S ACRONYM(S)
	11. SPONSOR/MONITOR'S REPORT NUMBER(S)

12. DISTRIBUTION/AVAILABILITY STATEMENT **Approved for public release, distribution unlimited**

13. SUPPLEMENTARY NOTES **The original document contains color images.**

14. ABSTRACT

15. SUBJECT TERMS

16. SECURITY CLASSIFICATION OF:			17. LIMITATION OF ABSTRACT	18. NUMBER OF PAGES	19a. NAME OF RESPONSIBLE PERSON
a. REPORT **unclassified**	b. ABSTRACT **unclassified**	c. THIS PAGE **unclassified**	**UU**	**10**	

Fig. 1. An experiment in progress at the LSTF

Four wave generators were used to produce waves in the LSTF. The generators are synchronized to produce unidirectional long-crested waves at a 10-deg angle to shore normal. A digitally controlled drive servo electric system controls the position of the piston-type wave board, and produces waves with the periodic motion of the board. The system allows a variety of regular and irregular wave types to be produced. The generators were oriented at a 10-deg wave angle for the present study, but they can be positioned to produce waves from 0 to 20 deg from shore normal.

The beach was constructed using approximately 150 m^3 of fine quartz sand having a median grain diameter, d_{50}, of 0.15 mm. It was desired to obtain an accurate rate of longshore sediment transport and its cross-shore distribution with minimal longshore variation and boundary influences. Therefore, straight and parallel contours were maintained throughout the model to maximize the length of beach over which longshore uniformity of waves and currents exist in the basin. Beaches having "three-dimensionality" affect incident waves and, subsequently, the longshore currents and sediment transport associated with the waves.

The model beach was of finite length and bounded at the upstream and downstream ends. To minimize adverse laboratory effects created by the boundaries and to produce uniform longshore currents across the beach, it was necessary to supplement wave-driven currents. A recirculation system was installed which consisted of 20 independent vertical turbine pumps placed in the cross-shore direction at the downdrift boundary. Flow channels were placed upstream of each pump to direct flow to the pump, which externally re-circulated the current to the upstream end of the facility, where it was discharged through flow channels onto the beach. The objective of this system was to maximize the length of beach

Smith and Wang

over which waves and wave-driven longshore currents are uniform by continually re-circulating wave-driven longshore current through the lateral boundaries of the facility. Each pump included a variable speed motor to control discharge rates. The variable speed motors were controlled remotely to allow a cross-shore distribution of longshore current.

A 21-m instrumentation bridge spanned the entire cross-shore of the beach and served as a rigid platform to mount instruments and observe experiments. Each end of the bridge was independently driven on support rails by drive motors, which allowed it to travel the entire length of the wave basin. The bridge could be moved either manually or by entering the desired longshore (Y) location on a PC in the LSTF control room.

INSTRUMENTATION

Time series of water surface elevations was measured using single-wire capacitance-type wave gauges. Ten gauges were mounted on the instrumentation bridge to provide wave heights as they transformed from offshore to nearshore. The cross-shore location of the gauges could be repositioned on the bridge depending on the wave conditions. Additionally, four gauges were placed in front of each wave generator to measure offshore wave characteristics.

Ten acoustic doppler velocimeters (ADVs) were used to measure orbtal wave velocities and unidirectional longshore currents. The ADVs were positioned at the same cross-shore position on the bridge with the wave gauges, but separated by approximately 40 cm in the longshore direction to prevent interference between the two instrument types. As with the wave gauges, the ADV cross-shore location could be repositioned on the bridge.

The eight most offshore ADVs were down-looking three-dimensional (3D) sensors, which sampled velocities in the x, y, and z directions 5 cm below the sensor. The first two ADVs were two-dimensional (2D) side-looking sensors, which sampled velocities in the x and y directions, also 5 cm from the sensor. The 2D sensors were used to allow measurements in water too shallow for the 3D current meters.

All of the ADVs were mounted on vertical supports that allowed the vertical position of the sampling volume to be adjusted. Typically, the ADVs were positioned vertically to sample at a location that gave the average velocity in the water column. However, some experiments were conducted in which the vertical position of the ADVs was varied to obtain the velocity distribution through the water column.

An automated beach profiler mounted to the instrumentation bridge was used to survey the beach. A mechanical spring-wheel system attached to a vertically mounted rod followed the sand elevation as the system moved cross-shore along the bridge. The vertical movement of the rod produced a voltage, which was recorded and converted to elevation. The vertical resolution of the system was ±1 mm. Horizontal positioning of the profiler was controlled by the bridge position and a cross-shore motor mounted on the bridge. The profiling system was amphibious to allow the entire beach to be surveyed without draining the basin.

Survey data were obtained every 5mm in the cross-shore direction and every 0.5 or 1.0 m in the longshore direction. Initially, survey lines were taken every 0.5 m in the

longshore; however, the middle portion of the beach remained uniform and the higher resolution was not required. Higher irregularity in the bathymetry occurred near the upstream and downstream boundaries, and denser profile lines were required.

Twenty traps were installed in the downdrift flow channels to collect sand transported through the downdrift boundary. Seventeen traps were placed in the flow channels of the first 17 pumps, and one trap was placed in the flow channel of pump 19. Traps were omitted from channels 18 and 20 because sediment transport was expected to be low in the offshore region. The remaining two traps were placed in the swash zone.

To determine the cross-shore distribution of longshore sediment transport, each sand trap was equipped with three load cells to weigh the amount of trapped sand. The total capacity of the 20 traps is 2500 kg. As experiments progressed, the updrift end of the beach became depleted of sand. It was necessary to dredge the traps to replenish the updrift portion of the beach, and rebuild the beach to uniform and parallel contours.

LONGSHORE TRANSPORT EXPERIMENTS

Longshore transport experiments were conducted for two breaker types with the wave conditions given in Table 1. Zero-moment wave height, H_{mo}, water depth, h, and incident wave angle, θ, were the same in both cases, and only the peak wave period, Tp, varied.

Table 1. Longshore Sediment Transport Experiment Wave Conditions

Breaker Type	H_{mo} m	T_p sec	h m	θ deg
Spilling	0.247	1.5	0.9	10
Plunging	0.247	3.0	0.9	10

Uniformity of Longshore Currents

The first step of the experiments was to determine the distribution of wave-induced longshore current. Visser (1991) determined from laboratory experiments that if the re-circulated currents either exceeded or were less than the wave-driven currents, an internal current would develop and re-circulate within the offshore portion of the basin. Visser also found that as the pumped currents approached the proper current, the internally re-circulated current was minimized. Therefore, it was desired to match wave-driven currents with pumped currents. Initial pumps were based on results of the numerical model NMLONG (Kraus and Larson 1991), and the iterative approach described by Hamilton and Ebersole (2001) and Hamilton, et al. (2001) was used to determine the optimum pump settings. After the beach had reached an equilibrium or quasi-equilibrium profile, and the pumped currents matched measured velocities, experiments on longshore transport rate were initiated. Spilling breakers required 1,330 minutes to reach equilibrium in the model and plunging breakers reached equilibrium after 280 minutes of wave action.

Results

Figure 2 shows the transformation of waves from offshore to nearshore. Spilling waves show a fairly gradual decrease in wave height across the beach. Plunging breakers shoal farther shoreward and the break point is evident where wave height sharply decreases. The corresponding equilibrium beach profiles formed by the two wave types are shown in Figure 3. The profile associated with spilling breakers consists of three near-planar slopes. The offshore slope of the beach becomes gentle through the surf zone to the swash zone, and the slope becomes steep in the nearshore. A breakpoint bar and trough formed under plunging waves, and slight erosion occurred compared to the spilling wave case.
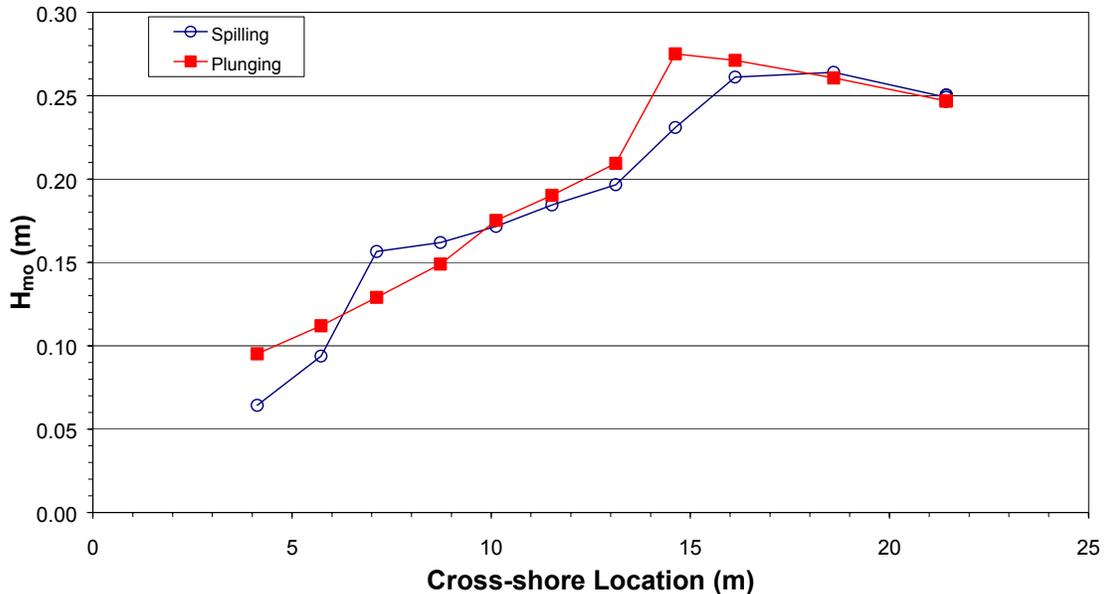

Fig 2. Wave transformation of spilling and plunging breakers

Average longshore current measured in the center portion of the beach for both wave cases is shown in Figure 4. The spilling case shows an upward trend towards the nearshore with a peak immediately seaward of the swash zone. Longshore currents associated with the plunging waves also show an increasing trend towards the nearshore. However, the plunging waves currents have a double peak in velocity; one at the break point and one in the swash zone. Although, measured velocities are slightly higher with plunging waves, the two cases have similar cross-shore distributions of longshore velocity.

Sediment flux was calculated from the rate of sand collected in each trap. Although the wave heights were identical for the two wave cases, and the resulting wave-driven longshore currents were similar, the sediment flux of the two breaker types is significantly different (Figure 5). The plunging wave case has peaks in transport at the break point and in the swash. A single peak occurs in transport with the spilling wave case in the swash zone.
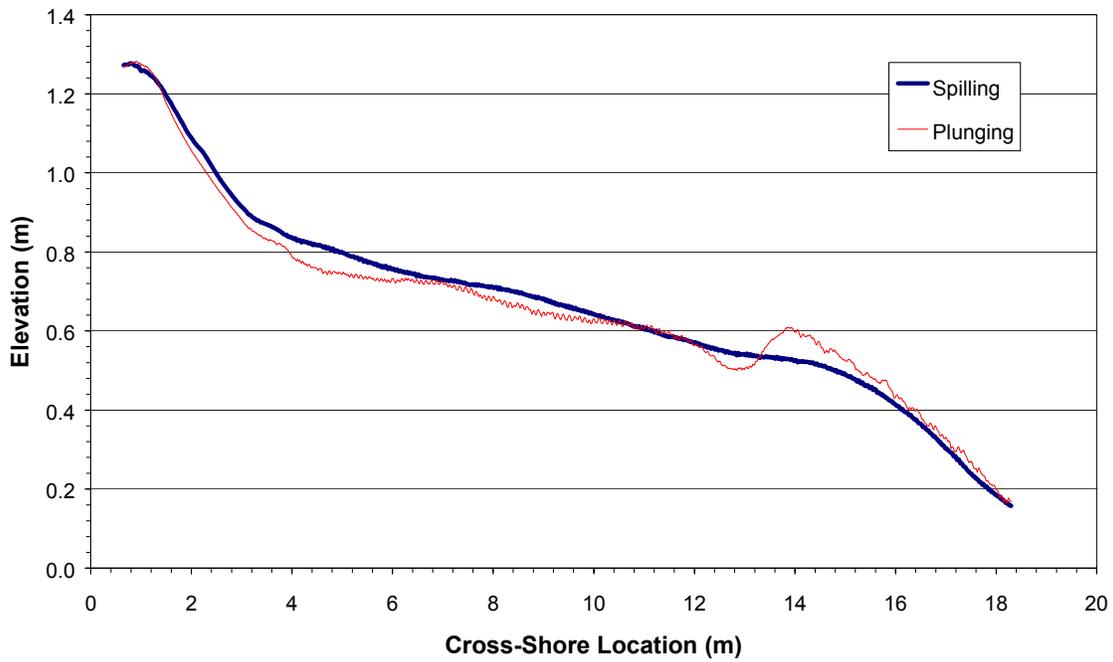
Smith and Wang

Fig 3. Equilibrium profiles formed by spilling and plunging breakers
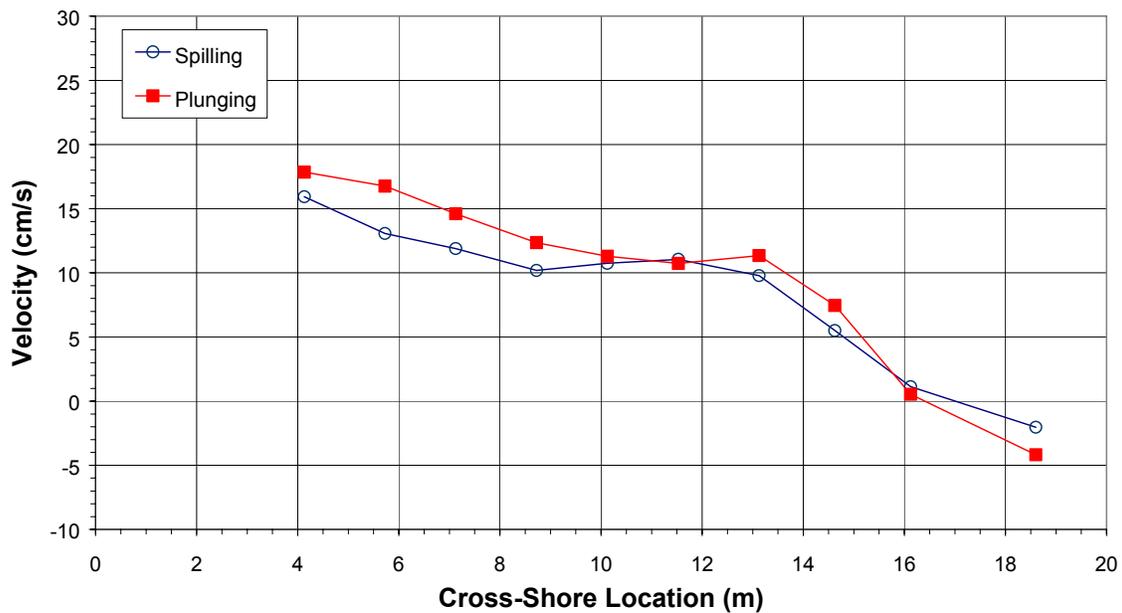

Fig. 4 Distribution of longshore currents produced by spilling and plunging waves

Total transport for spilling waves is approximately a third less than that of the plunging waves. Throughout the rest of the surf zone, sediment flux is similar between the cases.

It is not surprising that the plunging waves show greater transport over spilling waves near the breaker line. Turbulence associated with spilling breakers remains close to the
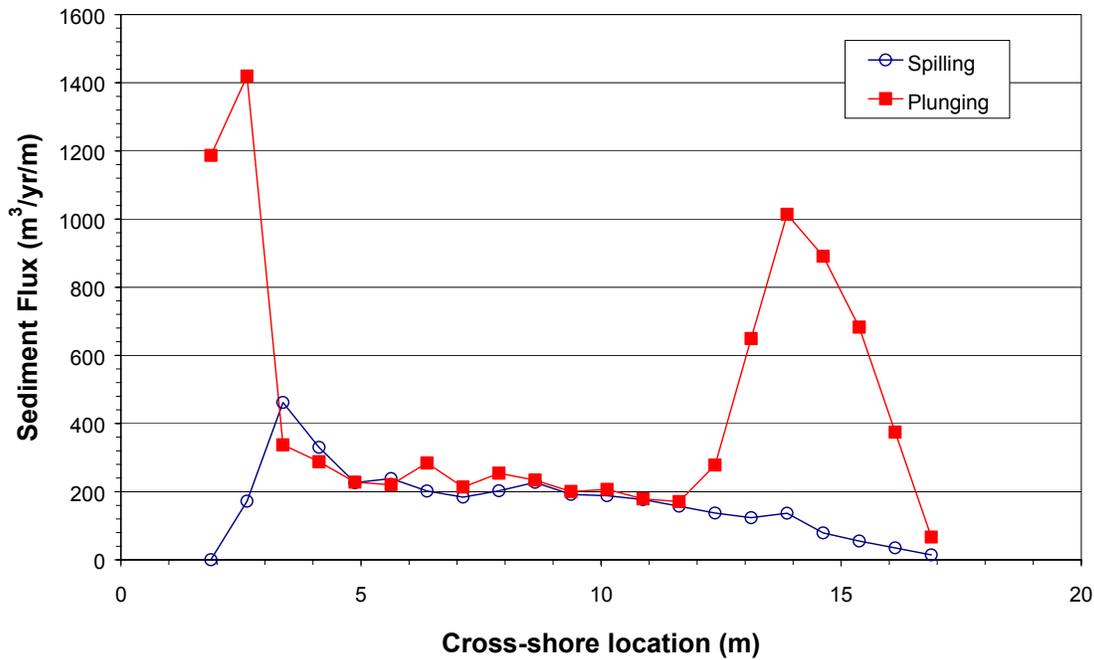
Smith and Wang

Fig. 5. Sediment flux distribution of spilling and plunging waves

surface in the bore. The jet associated with plungers penetrates deep into the water column and causes sand to be suspended and transported by the longshore current. Through the mid-surf zone, turbulence associated with broken plunging waves remains near the surface, and transport is similar between breaker types. However transport in the swash zone is substantially higher with plunging waves.

Comparison to Predictive Equations

Measured transport rates for the spilling and plunging case were compared to the CERC formula (Shore Protection Manual 1984), and predictive equations of Kamphuis, et al. (1986), Kamphuis (1991), and Kraus (1988). The CERC formula is given by:

$$I = \frac{K}{16\sqrt{\dfrac{H_b}{h_b}}} \rho g^{\frac{3}{2}} H_b^{\frac{5}{2}} \sin(2\theta_b) \tag{1}$$

in which I is the submerged weight transport rate, K is an empirical coefficient recommended by the Shore Protection Manual to be 0.39, H_b, h_b, and θ_b are wave height, water depth, and wave angle at breaking, respectively, ρ is fluid density, and g acceleration due to gravity.

Kamphuis, et al. (1986) developed an empirical equation based on field data as:

$$Q = 1.28 \frac{H_b^{3.5} m}{d} \sin(2\theta_b) \tag{2}$$

1224   Smith and Wang

in which Q is the total volume transport rate in kg/s, d is sediment grain size, and m is beach slope. . Kamphuis (1991) modified Equation 2 based on laboratory data and re-analysis of existing field data to include the influence of wave period and give Q in m^3/yr:

$$Q = 6.4x10^4 H_b^2 T_p^{1.5} m^{0.75} d^{-0.25} \sin^{0.6}(2\theta_b)$$ (3)

Kraus, et al. (1988) used a different approach and assumed that the total rate of longshore sediment transport in the surf zone is proportional to the longshore discharge of water. They found:

$$Q \propto K_d(R - R_c)$$ (4)

where K_d is an empirical coefficient that may relate to sediment suspension, R_c is a threshold value for significant longshore sand transport, and R is the discharge parameter, which can be accurately measured in the LSTF and calculated in the field as:

$$R = nV_{ls}x_b H_b$$ (5)

in which n is a constant, V_{ls} is the average longshore current velocity, and x_b is the surf-zone width. Based on field data, Kraus, et al. suggest $K_d = 2.7$ and $R_c = 3.9$ m^3/s.

Table 2 lists measured transport rates and the values of the predictive equations. The CERC equation over-predicts the total rate for spilling waves by over 700 percent and plunging waves by nearly 250 percent. It is interesting to note that the other equations may predict transport rate for one breaker type well, but none predict values that estimate both types well. In fact, with the exception of Kamphuis (1991), which includes wave period, the predictions do not reflect differences between breaker types.

Table 2. Comparison of Measured and Predicted Transport Rates

Transport Rates	Spilling Case m³/yr	Plunging Case m³/yr
Measured	2,660	7,040
CERC formula	22,030	23,850
Kamphuis (1986)	10,760	9,100
Kamphuis (1991)	2,200	5,360
Kraus (1988)	2,670	3,150

Measured sediment flux and an energy dissipation parameter were plotted as a function of cross-shore location for plunging and spilling breakers in Figures 6 and 7, respectively. The dissipation parameter was calculated by multiplying longshore velocity by the difference in energy, i.e., the difference in H^2, divided by distance between cross-shore measurement locations. Figure 6 shows a sharp increase in sediment flux corresponding to a peak in energy dissipation for plunging waves. Although dissipation is less for the spilling
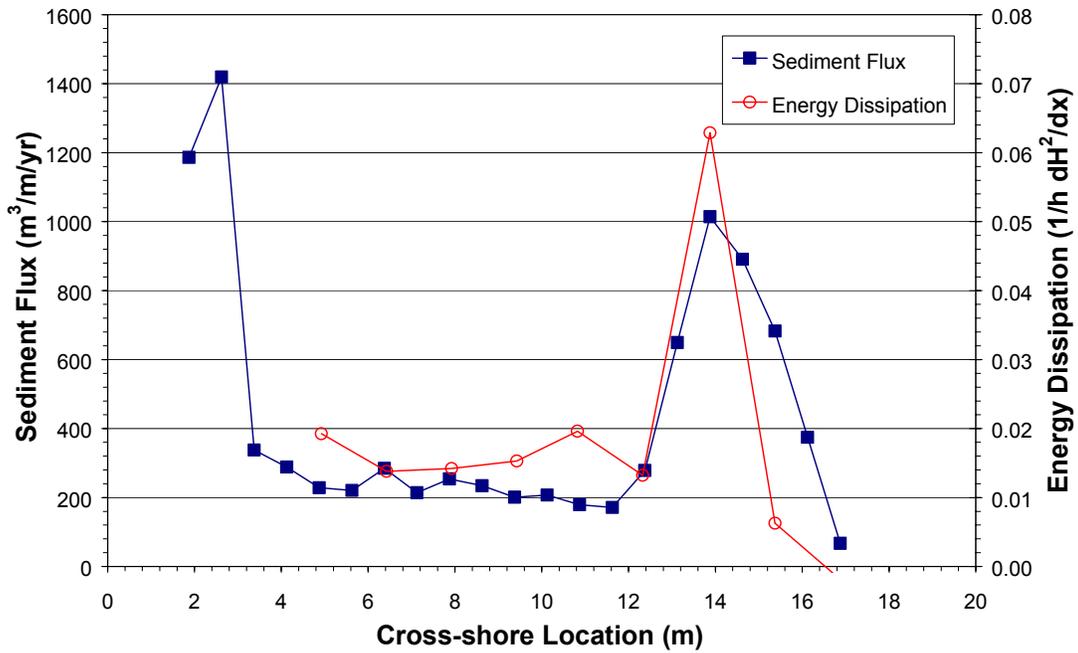
Fig. 6. Sediment flux and energy dissipation for plunging waves
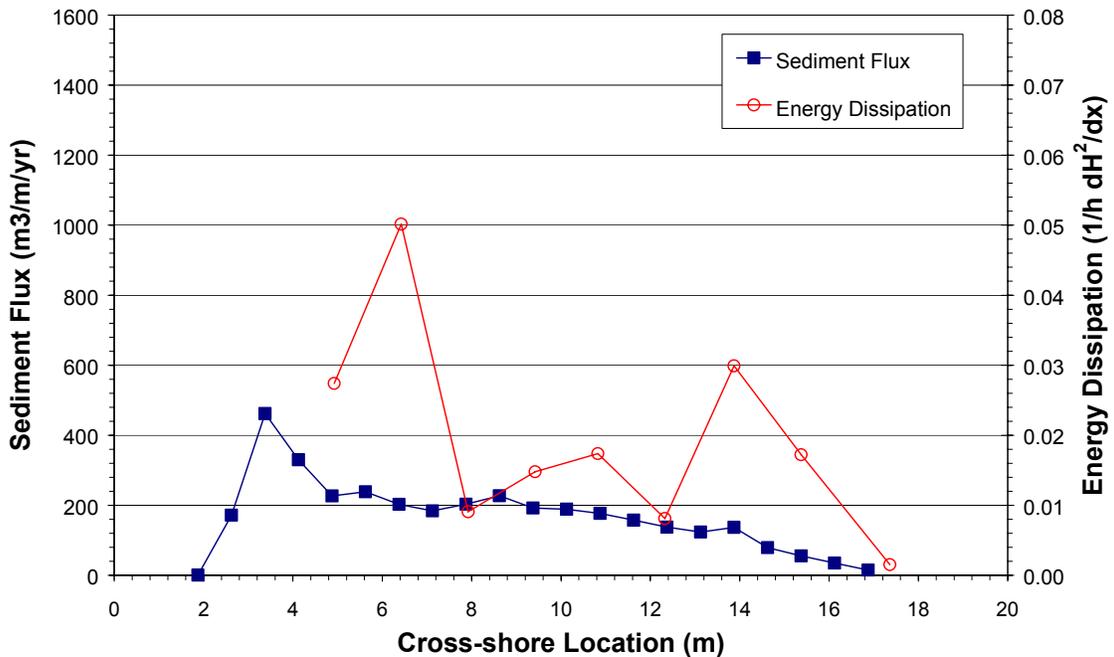

Fig. 7. Sediment flux and energy dissipation for spilling waves

waves, Figure 7 shows that sediment flux does not increase with a significant increase in energy dissipation.

The figures indicate that turbulence associated with plunging breakers penetrate to the sand bed and suspend sediment, which is transported by the longshore current. Higher energy dissipation with spilling waves did not produce an increase in sediment flux.

SUMMARY

Waves, currents, and sediment transport rate were measured in a large-scale physical model. Large differences were found in the cross-shore distribution and total sediment transport rates between spilling and plunging breakers. Existing predictive equations did not predict the total transport well and, with the exception of the Kamphuis (1991) equation, generally didn't differentiate between breaker types.

The data show that transport increases where wave energy dissipation is high with plunging breakers. High dissipation didn't necessarily produce increased transport rates with spilling breakers. Further study will be given to sediment transport as a function of breaker type, including additional experiments and comparisons to field data.

REFERENCES

Hamilton, D.G., Ebersole, B.A., Smith, E.R., and Wang, P., 2001. Development of a Large-Scale Laboratory Facility for Sediment Transport Research. *Technical Report*, U.S. Army Engineer Research and Development Center, Vicksburg, MS.

Hamilton, D.G., and Ebersole, B.A., 2001. Establishing Uniform Longshore Currents in a Large-Scale Laboratory Facility. *Coastal Engineering*, 42, 199-218.

Kamphuis, J.W., 1991. Alongshore Sediment Transport Rate. *Journal of Waterway, Port, Coastal and Ocean Engineering*, 117(6), ASCE, 624-641.

Kamphuis, J.W., Davies, M.H., Nairn, R.B., and Sayao, O.J., 1986. Calculation of Littoral Sand Transport Rate. *Coastal Engineering*, 10, 1-21.

Kraus, N. C., Gingerich, K.J., and Rosati, J.D., 1988. Toward an Improved Empirical Formula for Longshore Sand Transport. *Proceedings of 21st Coastal Engineering Conference*, ASCE, 1183-1196.

Kraus, N.C., and Larson, M., 1991. NMLONG: Numerical Model for Simulating the Longshore Current – Report 1: Model Development and Tests. *Techincal Report DRP-91-1*, U.S. Army Engineer Research and Development Center, Vicksburg, MS.

Shore Protection Manual, 1984. U.S. Army Engineer Waterways Experiment Station, U.S. Government Printing Office, Washington, D.C.

Visser, P. J., 1991. Laboratory Measurements of Uniform Longshore Currents. *Coastal Engineering*, 15, 563-593.